

APPLICATIONS OF PMW RAINFALL ALGORITHMS TO MEDITERRANEAN AREA EVENTS

F. Torricella¹, V. Levizzani¹, and V. Poli¹

¹Institute of Atmospheric Sciences and Climate, ISAC-CNR, Bologna, I-40121, Italy

1. INTRODUCTION

The application of passive microwave (PMW) and blended PMW-IR algorithms for satellite rainfall measurement is well established, especially if averaged or cumulated precipitation intensities are at stake. The application of operational global algorithms (GPROF, NESDIS, NRL) to specific case studies in complex orography regions as the Mediterranean demonstrates that regional applications are not viable without adapting the algorithms to the specific geographical area and season of the year. Often, in the *land* part of the algorithms, the initial screening that is supposed to discriminate the various surface types (ice, snow, desert, arid land) and precipitation seems to work only to a certain extent, being based on empirical global thresholds that hardly fit all specific local conditions. Cloudy and precipitating pixels can be erroneously classified as snow or ice contaminated and thereby discarded from the rain retrieval procedure altogether. Hereafter the analysis of two precipitation events occurred in the Mediterranean basin is presented, namely the storm on 4-5 December 2002 in the Antalya region (Turkey), and the November 2001 Algeria flood. Heavy rainfall events often occur during autumn and winter over the Central and Eastern Mediterranean, producing significant rain amounts and eventually leading to floods.

The present analysis demonstrates that in certain cases paying attention to the coastal environment and to pixel classification the overall performance of the methods can significantly improve. The rain maps are compared to nearly coincident time-space measurements taken from the precipitation radar (PR) onboard the Tropical Rainfall Measurement Mission (TRMM).

2. DATA AND ALGORITHMS

SSM/I measurements (brightness temperatures in 7 polarized channels from 19.2 to 85.5 GHz) available from the operational platforms F13, F14, and F15 were collected over the area. Data from the 1B11 operational algorithm of the TRMM Microwave Imager (TMI) were used. From these data, rain rates were derived by means of the NOAA-NESDIS operational algorithm (Ferraro and Marks 1995; Ferraro 1997) and

the Goddard Profiling Algorithm (GPROF) (Kummerow et al. 2001; McCollum and Ferraro 2003, and references therein). The NESDIS algorithm derives rainrates at the A-scan resolution of the SSM/I (~25 km) by means of non-linear relationships among the instrument channels (vertical and horizontal polarization) that have been calibrated using large sets of ground reference data collected by radar networks in different countries.

The latest GPROF algorithm (version 6) calculates instantaneous rainfall rate estimates from the weighted average of rainfall rates from different vertical hydrometeor profiles created from numerical cloud models, primarily the Goddard Cumulus Ensemble (GCE) model. Radiative transfer calculations using the frequencies and resolutions of a particular satellite are carried out to produce a library of vertical profiles with the associated brightness temperatures. The profiles used for estimation are chosen and given weights based on the proximity of the observed MW radiances to those of the library of profiles. An additional application of the profiles is in estimating latent heating profiles for model assimilation. The physical basis of the GPROF algorithm is most useful over oceans, where the low and predictable oceanic emissivity results in information about ice and liquid hydrometeors over the range of MW frequencies. The high and variable emissivity of the land surface makes the information from lower frequency channels more ambiguous, so that the ice scattering at higher frequencies is currently the most useful way to estimate rainfall over land.

The PR reference data were taken from the 2A25 official rain product (near surface rain variable).

3. CASE STUDIES

3.1 The 2001 Algeria Flood

In early November 2001 a widespread frontal system and upper air trough from northeast Scandinavia to southwest Spain led to an extreme precipitation event in Algiers, causing severe flooding and huge mudslides. More than 120 mm of rain fell in 12 h during the night between 9 and 10 November and more than 130 mm during the next 6 hours on the mountains behind Algiers. The unusually high rain rates were fed by the cold maritime arctic air that picked up moisture crossing the warm Mediterranean waters and met maritime subtropical air. An intense orographic enhancement was caused by strong surface winds oriented towards the high mountains of the African coast (> 2300 m a.s.l.).

Corresponding author's address: Francesca Torricella, Institute of Atmospheric Sciences and Climate ISAC-CNR, Bologna, I-40129, Italy; E-Mail: f.torricella@isac.cnr.it.

Due to the short duration of the event (about 20 h), the area was imaged only a few times by PMW instruments. The event was extensively studied in the past, with the disappointing result that, due to the particular combination of unfavorable conditions (precipitation in coastal environment, rapid onset of the event, no availability of ground reference data), no rain retrieval method based on satellite-based passive observations was able to detect rain over Algiers and its surroundings. The characteristics of the clouds and precipitation fields were definitely different over land (warm rain) with respect to the convective cells embedded in the storm system, which developed over the sea very immediately offshore. Very likely the orography played a major role, especially the relief south of Algiers, shaping a precipitating system that, although embedded in a larger field, was neither detected by PMW algorithms nor by blended PMW-IR techniques.

3.2 The 2002 Antalya Flood

On 4 and 5 December 2002 an intense storm swept the Antalya coastal region in Turkey leading to floods in the area. The 24-h accumulated rainfall ending at 1800 UTC on 5 December exceeded 72 mm and reached 153 mm at two stations in the area around the city of Antalya. The electric activity during this event was quite important.

On 0000 UTC, 4 December 2002, a surface low of 998 hPa was centered over southern Italy with a cold front spanning north to south over the Adriatic Sea. At 500 hPa a cut-off low of 5400 m was located slightly to the west of the surface low with the axis of the trough being oriented northwest-southeast. The Aegean Sea and the eastern – southeastern part of Turkey were under the influence of the diffluent trough. During the following 48 h the cut-off low stayed almost stationary without any deepening while only the axis of the trough slowly turned cyclonically dislocating the area of maximum diffluence over the southwestern part of Turkey. At the same time at surface levels the low pressure center was also stationary with a central pressure of 1000 hPa over southern Italy, while the associated cold front had progressed northeastwards also turning cyclonically and turned to an occluded front at 0000 UTC on 6 December.

4. RESULTS

In Fig. 1 the pixel-by-pixel classification for the Algeria case is presented for the TRMM orbit imaging the area around 0209 UTC on day 10, i.e. during the peak of the event. These results are taken from the GPROF classification, largely based on the work of Groody (1991) and Adler et al. (1994). It is apparent that in this case, the majority of land and coastal pixels is discarded prior the rain retrieval procedure, being classified as contaminated by the presence at the surface of ice or desert, or flagged as certainly non-raining. The comparison with the coincident IR image

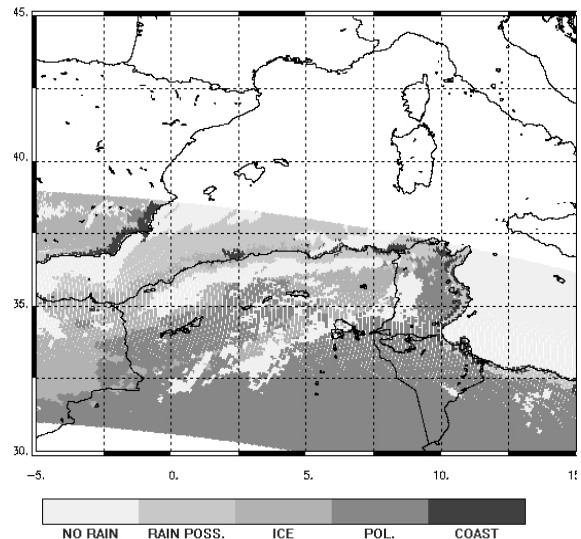


Figure 1. Pixel classification for the TRMM orbit #22742 (overpass time 0209 UTC, November 10) from GPROF6 applied to TMI brightness temperatures.

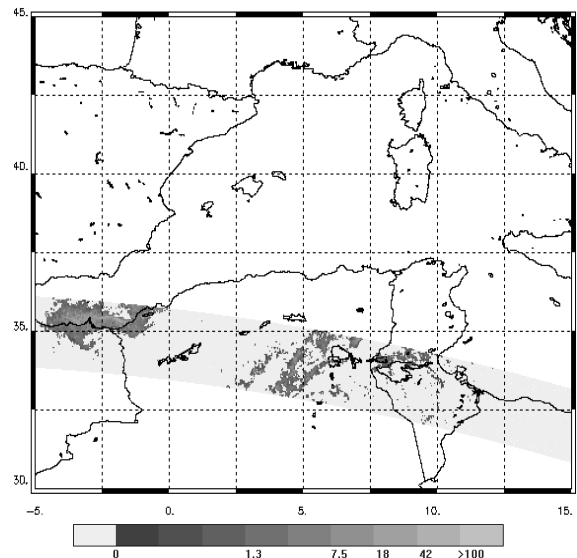


Figure 2. Rain map (in mm h^{-1}) for the same orbit of Fig. 1 derived from the 2A25 PR operational product.

of the VIRS spectrometer (not show) reveals that the non-realistic ice detection is in reality connected with precipitating clouds, as confirmed by the PR (Fig. 2).

In Fig. 3 the results of GPROF upon application of the pixel analysis in Fig. 1 are shown, revealing that precipitation over land and the coastal area detected by the PR is missed altogether by the algorithm, as well as the very intense precipitation cells off the Morocco-Algeria coast. In Fig. 4 the TMI measurements are re-processed with GPROF after a correction of the screening procedure aimed at eliminating the ice flagging. It is evident that the new screening corrects the wrong attitude of the retrieval,

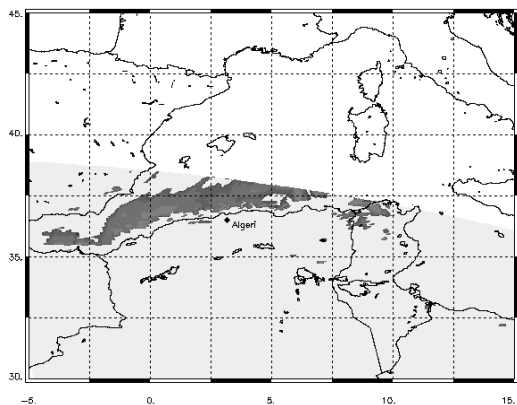


Figure 3. Rain map (in mm h^{-1}) for the same orbit of Fig. 1 derived from the from GPROF6 applied to TMI brightness temperature. Color palette as in Fig. 2.

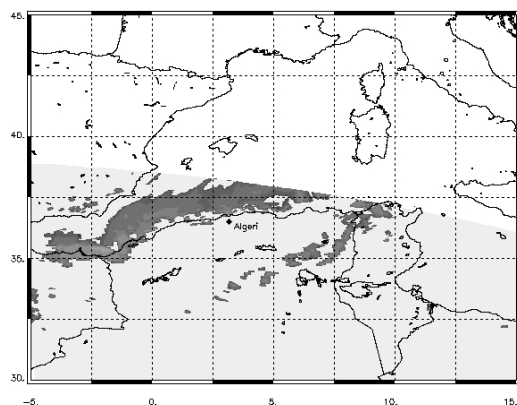


Figure 4. Same as in Fig. 3 but after correcting the pixel classification.

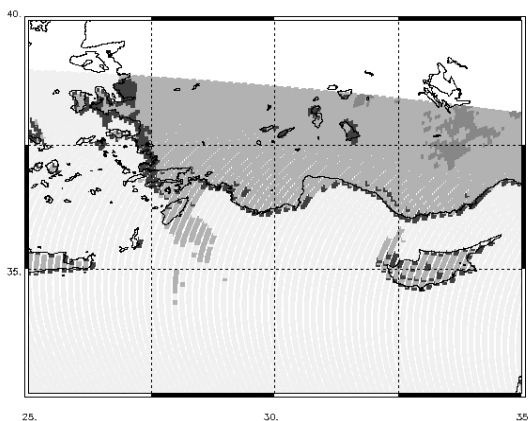


Fig. 5 Pixel classification for the TRMM orbit #28831 (overpass time 1808 UTC, December 5) from GPROF6 applied to TMI brightness temperatures.

and the convective precipitation off coast is detected. SSM/I overpasses (1919 and 1958 on day 9) processed by means of NESDIS algorithm (not shown) reveal very similar features in the precipitation

field and do not add relevant information for the analysis of the event.

The effect of the screening procedure for the Antalya case is shown in Fig. 5. Non-realistic features did not arise over this area, and the pixels classified as “rain-possible” fairly correlate with cloud features in the VIRS IR pictures (not shown). Nevertheless, the intrinsic weakness of PMW rain algorithms in locating and gauging rain in coastal zones shows up in comparing results with the PR data (see Fig. 6, unfortunately only marginal overpasses are available, due to the small PR swath). In PMW rain maps (Fig 6, left: TMI; Fig. 7 and 8: from SSM/I) the rain field shows unphysical discontinuities across the coastline, perhaps more evident in TMI data with respect to SSM/I’s.

5. REFERENCES

Adler, R. F., G. J. Huffman, and P. R. Keehn, 1994: Global tropical rain estimate from microwave adjusted geosynchronous IR data. *Remote Sens. Rev.*, **11**, 125-152.

Ferraro, R. R., 1997: Special sensor microwave imager derived global rainfall estimates for climatological applications. *J. Geophys. Res.*, **102** (D14), 16715-16735.

Ferraro, R. R., and G. F. Marks, 1995: The development of SSM/I rain-rate retrieval algorithms using ground-based radar measurements. *J. Atmos. Oceanic Technol.*, **12**, 755-770.

Grody, N. C., 1991: Classification of snow cover and precipitation using the Special Sensor Microwave Imager. *J. Geophys. Res.*, **96**, 7423-7435.

McCollum, J. R., and R. Ferraro, 2003: Next generation of NOAA/NESDIS TMI, SSM/I, and AMSR-E microwave land rainfall algorithms. *J. Geophys. Res.*, **108** (D8), 8382, doi:10.1029/2001JD001512.

Kummerow, C., Y. Hong, W. S. Olson, S. Yang, R. F. Adler, J. McCollum, R. Ferraro, G. Petty, and T. T. Wilheit, 2001: The evolution of the Goddard Profiling Algorithm (GPROF) for rainfall estimation from passive microwave sensors. *J. Appl. Meteor.*, **40**, 1801-1820.

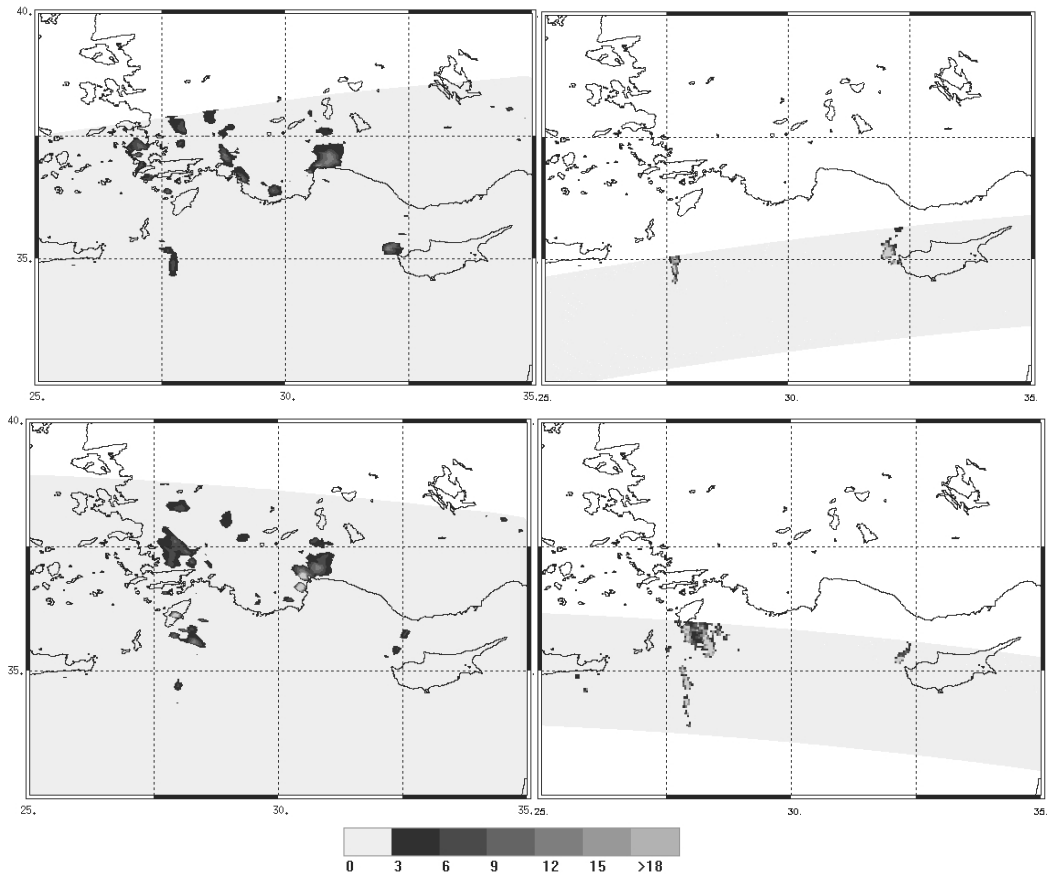


Fig. 6 Rain maps (in mm h^{-1}) derived by means of GPROF from TMI data (left), and from PR operational product 2A25 (right) for the TRMM orbit #28830 (top) and #28831 (bottom), on December 5.

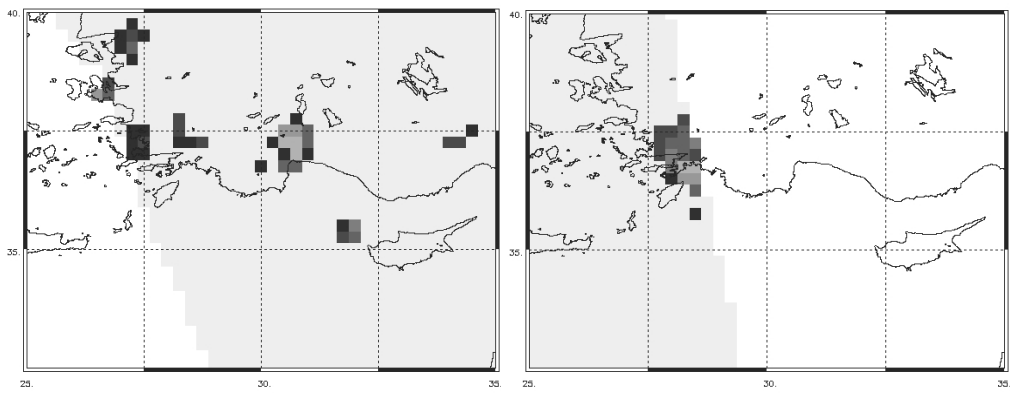


Fig. 7 Rain maps (in mm h^{-1}) derived by means of GPROF from SSM/I data. Left: orbit 1452-1538. Right: orbit 1858-1947. Color palette as in Fig. 6.